Journal of Inclusion Phenomena and Macrocyclic Chemistry (2019) 95:35–48
https://doi.org/10.1007/s10847-019-00892-z

ORIGINAL ARTICLE

QCM sensors coated with calix[4]arenes bearing sensitive chiral moieties for chiral discrimination of 1-phenylethylamine enantiomers

Egemen Ozcelik[1,2] · Farabi Temel[1,2] · Serkan Erdemir[3] · Begum Tabakci[3] · Mustafa Tabakci[1,2]

Received: 10 November 2018 / Accepted: 22 February 2019 / Published online: 1 March 2019

Abstract

This article describes the enantiomeric discrimination properties of new chiral calix[4]arene derivatives bearing (*S*)-/(*R*)-1-phenylethylamine moieties (**5a** and **5b**, respectively) towards the 1-phenylethylamine enantiomers on QCM surface. Initial experiments demonstrated that the **5b** coated QCM sensor was the most effective sensing material for enantiomeric discrimination of (*R*)-/(*S*)-1-phenylethylamine by exhibiting much more sensing ability towards (*R*)-enantiomer than (*S*)-enantiomer. Sensitivity, detection limit and time constant of the **5b** coated QCM sensor has been were calculated as 0.082 Hz/μM, 2.7 μM, and 319.2 s, respectively. Additionally, effects of calixarene content and different coating technique on enantiomeric discrimination, and Langmuir and Freundlich isotherms of the sensing results also were studied. As a result, it has been demonstrated that the coating of QCM sensor with a chiral calix[4]arene (**5b**) having (*S*)-1-phenylethylamine moieties provides substantially enantiomeric discrimination of 1-phenylethylamine enantiomers.

Keywords 1-Phenylethylamine · Organic coatings · Calixarene · Enantiomeric discrimination · Quartz crystal microbalance sensor

Introduction

One of the most common functional groups in chemistry is amines, and they are widely used in the production of synthetic materials, such as amino acids, alkaloids, pesticides and many commercial pharmaceuticals [1]. On the other hand, chiral amine pairs can cause different pharmaceuticals effect such as toxicity, activity, metabolic effect. For this reason, enantiomeric discrimination of chiral pairs is important phenomena in analytical chemistry investigations [2, 3]. For the sensing of chiral amines, it has been used and developed some analytical methods such as liquid chromatography [4], gas chromatography [5], UV–Vis [6], fluorescent [7], ^{1}H NMR [8], LSPR [9], potentiometric [10]. However, they have some disadvantages such as long time consuming and expensive analysis as well as their high investment cost and need for qualified staff. For these reasons, developments on technology lead to explore and use new sensor devices and methods such as acoustic systems for determination and detection of sensor material-analyte interaction in sensor applications [11, 12]. Among acoustic systems, QCM is an important technique to specify analytes at even low concentrations. The working principle of QCM related to changes at response depending on mass change on the quartz crystal. It includes a piezoelectric quartz crystal which has a sensitive and selective coating that serves as adsorptive surface [13]. There are many studies in the literature about QCM with sensing applications for biologic analytes such as carbohydrates, antibiotics, bacteria, DNA [14–17]. The relation between the mass of the adsorbed analyte and frequency shifting from fundamental frequency is defined as a mathematical equation as known as the Sauerbrey equation which can be expressed [18]:

$$\Delta F = -c_F \times \Delta m \quad (1)$$

Electronic supplementary material The online version of this article (https://doi.org/10.1007/s10847-019-00892-z) contains supplementary material, which is available to authorized users.

✉ Mustafa Tabakci
mtabakci@ktun.edu.tr; mtabakci@selcuk.edu.tr

[1] Department of Chemical Engineering, Konya Technical University, 42130 Konya, Turkey

[2] Department of Chemical Engineering, Selçuk University, 42130 Konya, Turkey

[3] Department of Chemistry, Selçuk University, 42130 Konya, Turkey

where ΔF is the observed frequency change in Hz, Δm is the change in mass per unit area in g cm^{-2} on quartz, C_F is the sensitivity factor for the crystal (56.6 Hz μ^{-1} cm^2 for a 5 MHz AT-cut quartz crystal at room temperature).

Third major generation of supramolecular host systems after crown ethers and cyclodextrins is calixarenes which are formed of phenolic units linked through the ortho positions. They can be easily available by condensation of *p-tert*-butylphenol with formaldehyde [19]. Furthermore, they can be readily functionalized and modified which caused that they have drawn interest in the host–guest chemistry. They were widely used for promising materials for sensor applications due to their sensing abilities and sensitivities [20–22].

Though calixarenes have been used for many applications there are limited studies using calixarenes as a sensor material for chiral amine pairs by QCM system in the literature. Hence, we have considered that the preparation of new chiral calix[4]arene platforms bearing chiral amine or amino alcohol moieties on their upper rim and disulfide on lower rim positions as the sensing materials to deposit onto QCM surface through the self assembling, and the application of these new chiral calix[4]arene coated QCM sensors to enantiomeric separation of the 1-phenylethylamine (PEA) enantiomers ((*R*)-/(*S*)-PEA) depicted in Fig. 1. Enantiomers of PEA can be widely used as key building blocks or precursor due to its low prices in a number of pharmaceutical and agromedical industry where need high purity and large quantities compounds [23–25]. For this reason, enantiomeric separation of PEA plays an important role in the preparation of enantiomerically pure compounds.

Initial experiments clearly revealed that the chiral calix[4]arene **5b** coated QCM sensors exhibited a good enantiomeric discrimination for PEA enantiomers by the evaluation of sensor responses [20] and enantiomeric discrimination factor (α) [26]. In further studies, different concentrations of PEA enantiomer solutions were studied to specify the effect of the concentration changes on enantiomeric discrimination. Thus, detection limit (DL) [27], sensitivity (S) [28], the time constant (τ) [29] were calculated, and Langmuir and Freundlich isotherm models were also applied to the data. On the other hand, the effects of the calixarene content and deposition technique on enantiomeric discrimination were performed in detail.

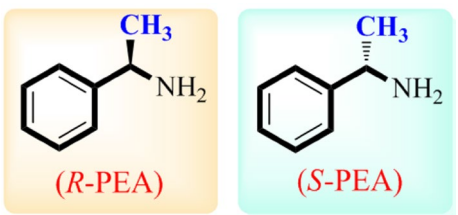

Fig. 1 Investigated 1-phenylethylamines

Experimental

Reagents and instrumentations

A Stuart-SMP3 apparatus in a sealed capillary was performed to find out all melting points of the synthesized calix[4]arene compounds. Structure determinations of all synthesized chiral calix[4]arene compounds were performed by A Varian 400 MHz NMR spectrometer, a Perkin Elmer 100 FTIR spectrometer, and an elemental analyzer branded with Leco CHNS-932. Analytical TLC was performed due to monitor the reactions using precoated silica gel plates (SiO_2 Merck F_{254}). All reagents using for the preparation of compounds and sensing applications were standard analytical grade from Merck, Sigma-Aldrich, Fluka and used without further purification.

A time-resolved QCM 200 was purchased from SRS (California, USA) to measure the frequency change of quartz crystals between gold electrodes. QCM crystals were cleaned within an ultrasonic bath (Isolab) by chloroform and distilled water, respectively. After every cleaning treatment, crystals were subjected to ultra pure nitrogen to supply their dryness. AFM images of coated and uncoated QCM surfaces were taken by NTEGRA Solaris atomic force microscope (NT-MDT, Moscow, Russia) at room temperature in air. Standard 125-μm long NSG30 silicon cantilevers (NT-MDT) with a force constant of 22–100 N m^{-1} were used. The typical curvature radius of the tip-cantilever was approximately 10 nm. Topographic images were captured in semi-contact mode with a resonance frequency of 240–440 kHz. The scanning speed was a 255 × 255 line. To determine the root mean square roughness values, AFM images were processed with Nova RC software (NT-MDT). Contact angles of QCM sensor surfaces were specified by DSA 25 from Krüss (Hamburg, Germany). Chiral calix[4]arene derivatives were deposited on QCM crystal surface by Laurell Technologies Corporation Spin Coater model WS-400BZ-6NPP/LITE. An ISM940E peristaltic pump from Ismatech (Wertheim, Germany) was used to pass the analyte solutions through the sensor surface. All experiments were performed in Labconco-5220120 glove box (Kansas City, MO, USA).

Synthesis

The synthesis of *p-tert*-butylcalix[4]arene (**1**) and its derivative **2** was synthesized according to previously published procedures, respectively [30, 31]. Other calix[4]arene compounds **3, 4** and chiral calix[4]arene derivatives (**5a** and **5b**) were synthesized by adapting known synthetic procedures for the first time.

Compounds 3

Compound **2** (1 g, 1.12 mmol) and thiourea (0.85 g, 11.20 mmol) in dry acetonitrile (100 mL) were stirred at reflux for a day. After that, KOH (0.89 g, 22.40 mmol) solved in deionized water (20 mL) was added in to the cooled reaction mixture. The mixture was stirred at room temperature for 2 h. After the reaction was completed, most of solvent was evaporated under reduced pressure. The remaining part was neutralized by 1 M HCl. The mixture was extracted by 2 × 40 mL CH_2Cl_2. The organic layer was dried over $MgSO_4$ and evaporated to give compound **3** (80%) as a white powder. mp: 190 °C. ^{1}H-NMR (400 MHz, $CDCl_3$): δ (ppm) 8.45 (s, 2H), 7.05 (s, 4H, ArH), 7.03 (s, 4H, ArH), 4.25 (d, 4H, J = 13.1 Hz, $ArCH_2Ar$), 4.11 (t, 4H, OCH_2), 3.45 (m, 4H, CH_2S), 3.39 (d, 4H, J = 13.1 Hz, $ArCH_2Ar$), 2.40 (brs, 4H, $OCH_2CH_2CH_2$), 1.26 (s, 18H, But), 1.15 (s, 18H, But). ^{13}C-NMR ($CDCl_3$, 100 MHz): δ (ppm) 28.43 ($OCH_2\boldsymbol{C}H_2CH_2S$), 30.51 ($ArCH_2Ar$), 31.18, 31.68 ($C(\boldsymbol{C}H_3)$), 32.38 ($OCH_2CH_2\boldsymbol{C}H_2S$), 33.83, 34.19 ($\boldsymbol{C}(CH_3)$), 74.65 ($O\boldsymbol{C}H_2CH_2CH_2S$), 125.41 (ArC-*m*), 125.86 (ArC-*o*), 127.18 (ArC-*m*), 133.00 (ArC-*o*), 141.71, 147.38 (ArC-*p*), 149.33, 150.82 (ArC-O). Anal. Calcd for $C_{50}H_{66}O_4S_2$: C, 75.52; H, 8.37; S, 8.06. Found: C, 75.21; H, 8.49; S, 8.19.

Compounds 4

Compound **3** (1.0 g, 1.26 mmol) and hexamethylenetetramine (HMTA, 7.06 g, 50.40 mmol) were taken in trifluoroacetic acid (TFA, 50 mL). The reaction mixture was refluxed until the starting material (compound **3**) had disappeared (TLC). Upon completion, the reaction mixture was cooled to room temperature and adding 1.0 M HCl (100 mL). Resulting mixture was extracted with dichloromethane (2 × 40 mL). The organic layer was washed with water three times and saturated brine once, and dried over $MgSO_4$. Removing the solvent after filtration gave to compound **4** in 70% yield. mp:182 °C [32]. ^{1}H-NMR (400 MHz, $CDCl_3$): δ (ppm) 9.77 (s, 2H), 9.47 (s, 2H), 7.63 (s, 4H, ArH), 7.04 (s, 4H, ArH), 4.22 (d, 4H, J = 13.1 Hz, $ArCH_2Ar$), 4.14 (t, 4H, OCH_2), 3.53 (d, 4H, J = 13.1 Hz, $ArCH_2Ar$), 3.41 (t, 4H, CH_2S), 2.42 (brs, 4H, $OCH_2CH_2CH_2$), 1.11 (s, 18H, But). ^{13}C-NMR ($CDCl_3$, 100 MHz): δ (ppm) 28.40 ($OCH_2\boldsymbol{C}H_2CH_2S$), 30.50 ($ArCH_2Ar$), 31.22 ($C(\boldsymbol{C}H_3)$), 31.87 ($OCH_2CH_2\boldsymbol{C}H_2S$), 34.33 ($\boldsymbol{C}CH_3$), 75.04 ($O\boldsymbol{C}H_2CH_2CH_2S$), 126.39 (ArC-*m*), 128.49, 128.90 (ArC-*o*),131.02 (ArC-*m*), 131.72, 148.60 (ArC-*p*), 149.09, 159.50 (Ar-C-O), 190.94 (C=O). Anal. Calcd for $C_{44}H_{50}O_6S_2$: C, 71.51; H, 6.82; S, 8.68. Found: C, 71.73; H, 6.72; S, 8.49.

Synthesis of chiral calix[4]arene derivatives (5a, 5b)

The synthesis of calix[4]arene derivatives (**5a** and **5b**) were carried out as following the general procedure: (*R*)-(+)-1-phenylethylamine, (*S*)-(−)-1-phenylethylamine were added to a solution of **4** (0.50 g, 0.68 mmol) dissolved in CH_3Cl (20 mL). After the mixtures were refluxed for 48 h in the presence of $MgSO_4$, it was filtered to remove $MgSO_4$. The solvents were evaporated and the solid residues were recrystallized with CH_3Cl/hexane (for **5a** and **5b**) to give as colorful crystals.

5a; Yield 62%; mp: 159–161 °C; ^{1}H-NMR (400 MHz, $CDCl_3$): δ (ppm) 8.98 (s, 2H), 8.16 (s, 2H), 7.58 (d, 1H, J = 1.95 Hz, ArH), 7.19–7.40 (m, 15H, ArH, Ph), 7.10 (d, 1H, J = 2.34 Hz, ArH), 7.05 (d, 1H, J = 2.34 Hz, ArH), 4.46 (q, 2H, $CHCH_3$), 4.24 (d, 2H, J = 12.5 Hz, $ArCH_2Ar$), 4.19 (d, 2H, J = 12.5 Hz, $ArCH_2Ar$), 4.12 (t, 4H, OCH_2), 3.48 (d, 4H, J = 13.1 Hz, $ArCH_2Ar$), 3.41 (brs, 4H, CH_2S), 2.41 (brs, 4H, $OCH_2CH_2CH_2$), 1.57 (d, 6H, $CHCH_3$), 1.14 (s, 18H, But). ^{13}C-NMR ($CDCl_3$, 100 MHz): δ (ppm) 24.46 (CH_3), 28.39 ($OCH_2\boldsymbol{C}H_2CH_2S$), 30.63 ($ArCH_2Ar$), 31.24 ($C(\boldsymbol{C}H_3)$), 31.93 ($OCH_2CH_2\boldsymbol{C}H_2S$), 34.32 ($\boldsymbol{C}(CH_3)$), 69.00 ($Ph\boldsymbol{C}H$), 74.94 ($O\boldsymbol{C}H_2CH_2CH_2S$), 125.72, 125.96 (PhC-*o*), 126.29, 126.36 (PhC-*p*), 126.42, 126.51 (ArC-*m*), 127.92, 128.05 (ArC-*o*), 128.24, 128.33 (PhC-*m*), 128.51, 128.58 (ArC-*o*), 129.36 (ArC-*p*), 132.46, 132.71 (ArC-*m*), 145.55 (ArC-*p*), 148.06 (PhC), 149.30, 155.61 (ArC-O), 159.56 (C=N). Anal. Calcd for $C_{44}H_{50}N_2O_6S_2$: C, 76.23; H, 7.25; N, 2.96; S, 6.78. Found: C, 76.39; H, 7.11; N, 3.01; S, 6.52.

5b; Yield 61%; mp: 163–165 °C; ^{1}H-NMR (400 MHz, $CDCl_3$): δ (ppm) 8.97 (s, 2H), 8.15 (s, 2H), 7.58 (d, 1H, J = 1.95 Hz, ArH), 7.19–7.40 (m, 15H, ArH, Ph), 7.10 (d, 1H, J = 2.34 Hz, ArH), 7.05 (d, 1H, J = 2.34 Hz, ArH), 4.46 (q, 2H, $CHCH_3$), 4.23 (d, 2H, J = 12.5 Hz, $ArCH_2Ar$), 4.18 (d, 2H, J = 12.5 Hz, $ArCH_2Ar$), 4.12 (t, 4H, OCH_2), 3.47 (d, 4H, J = 13.1 Hz, $ArCH_2Ar$), 3.42 (brs, 4H, CH_2S), 2.40 (brs, 4H, $OCH_2CH_2CH_2$), 1.56 (d, 6H, $CHCH_3$), 1.13 (s, 18H, But). ^{13}C-NMR ($CDCl_3$, 100 MHz): δ (ppm) 24.45 (CH_3), 28.39 ($OCH_2\boldsymbol{C}H_2CH_2S$), 30.63 ($ArCH_2Ar$), 31.24 ($C(\boldsymbol{C}H_3)$), 31.92 ($OCH_2CH_2\boldsymbol{C}H_2S$), 34.32 ($\boldsymbol{C}(CH_3)$), 69.01 ($Ph\boldsymbol{C}H$), 74.94 ($O\boldsymbol{C}H_2CH_2CH_2S$), 125.72, 125.97 (PhC-*o*), 126.29, 126.36 (PhC-*p*), 126.42, 126.51 (ArC-*m*), 127.92, 128.05 (ArC-*o*), 128.24, 128.33 (PhC-*m*), 128.51, 128.58 (ArC-*o*), 129.36 (ArC-*p*), 132.46, 132.72 (ArC-*m*), 145.55 (ArC-*p*), 148.05 (PhC), 149.30, 155.62 (ArC-O), 159.57 (C=N). Anal. Calcd for $C_{44}H_{50}N_2O_6S_2$: C, 76.23; H, 7.25; N, 2.96; S, 6.78. Found: C, 76.33; H, 7.08; N, 2.95; S, 6.66.

Preparation of QCM sensors

Baseline frequencies of sensor surface were recorded before the coating of calixarene molecules. For the coating, soaking technique was used as following procedure; 1.0 mM of

chiral calix[4]arene (**5a** and **5b**) solutions were prepared in chloroform, and this solution (3 µL) was injected the clean QCM crystal surfaces existed in a beaker and subsequently the solvents evaporated overnight. Thus, the chiral calix[4] arene coated QCM sensors were obtained. Last frequency values were recorded to determine the amount of coated chiral calix[4]arene on the surface.

Enantiomeric discrimination of PEA enantiomers

Chiral calix[4]arene coated QCM sensors were placed in QCM holder which was mounted by QCM flow cell. Later, distilled water was circulated in QCM flow cell by peristaltic pump to keep zero level frequency response for stabilization of sensors. In water, the dominant source of frequency drift comes from the temperature dependence of the viscosity of the liquid. The series resonant frequency of a 5 MHz AT-cut crystal in water will increase by about 8 Hz $^{\circ}C^{-1}$. For the elimination of temperature effect, the analytes were prepared by water which has the same temperature and all experiments were performed at 20 °C by way of glove box unit. After 200 µM PEA enantiomer solutions which were prepared in distilled water were circulated in QCM flow cell by a peristaltic pump. ΔF values of QCM sensors were recorded as a function of time continuingly during the circulation of PEA enantiomer solutions in sensing system. The resonance frequency decreased by adsorption of PEA molecules on QCM sensor surfaces. After sensing processes, sensor surfaces were subjected to distilled water for desorption of sensor surfaces due to break down interaction between chiral calix[4]arene and PEA molecules.

Results and discussion

Synthesis and characterization

We have interested in the synthesis of new Schiff base functionalized calix[4]arene derivatives (**1–4** and **5a, 5b**) having chiral binding sites such as amine in order to see their enantiomeric discrimination abilities towards PEA enantiomers through the QCM method. Hence, some calix[4]arene derivatives depicted in Scheme 1 were synthesized, and their structures were characterized by a combination of FT-IR, ^{1}H, and ^{13}C NMR spectroscopy. After the **1** and **2** were synthesized according to previous literature methods [30, 31], **2** was reacted with thiourea in dry acetonitrile to give **3** in 80% yield. The synthesis of **3** was confirmed by the appearance proton and carbon peaks of CH_2S-S at 3.45 and 32.38 ppm in the ^{1}H and ^{13}C NMR spectra, respectively [see Electronic Supplementary Material (ESM), Fig. S1 and S2]. Compound **3** was converted to its aldehyde derivative **4** in 70% yield by using hexamethylenetetramine in trifluoroacetic acid. The formation of **4** was confirmed by the appearance of the characteristic aldehyde C=O band at about 1682 cm^{-1} in its FT-IR spectra (see ESM, Fig. S3). The synthesis of **4** was also confirmed by the appearance of aldehyde proton and carbon peaks (HC=O) at 9.77 and 190.94 ppm in the ^{1}H and ^{13}C NMR spectra, respectively (see ESM, Fig. S4 and S5). The reaction of compound **4** with (*R*)-(+)-1-phenylethylamine and (*S*)-(−)-1-phenylethylamine in chloroform gave target chiral calix[4]arene derivatives **5(a/b)** in 62%, and 61% yields, respectively. The formation of **5(a/b)** was confirmed by the disappearance of characteristic aldehyde C=O band from derivative **4** and appeareance of characteristic imine C=N at about 1675 cm^{-1} in its FT-IR spectra (see ESM, Figs. S6, S7). Their structures were also confirmed by the appearance of Schiff base (HC=N) protons at 8.16, and 8.15 ppm and Schiff base (HC=N) carbons at 155.61, and 155.62 ppm, and disappearance of proton and carbon peaks belongs to aldehyde group at 9.77 and 190.94 ppm in ^{1}H and ^{13}C NMR spectrum of **4**, respectively (see ESM, Figs. S8, S9, only one NMR spectrum was given for each chiral pair).

Enantiomeric discrimination assays

New calix[4]arene derivatives **5(a/b)** having chiral binding sites were deposited on QCM gold surface to fabricate chiral calix[4]arene coated QCM sensors by soaking technique. In this step, disulfide moieties of **5(a/b)** can be strongly adsorbed on the gold surface to afford stable and ordered layers due to the bond formation between gold and sulfur. These QCM sensors have been used in sensing and enantiomeric discrimination assays of PEA enantiomers to specify the chiral calix[4]arene derivatives which can be effective and selective sensing material. A home-made sensing system, which was used in this study was shown in Fig. 2. The frequency changes (−ΔHz, it indicates to the response of QCM sensor) and enantiomeric discrimination factor (α) of **5(a/b)** modified QCM sensors towards PEA enantiomers were given in Table 1.

Enantiomeric discrimination factors (Table 1) were calculated through the resonance frequency shifts (Table 1) in response to PEA enantiomers by Eq. (2):

$$\alpha = \frac{\Delta F_R}{\Delta F_S} \tag{2}$$

where ΔF_R and ΔF_S are frequency changes of QCM sensors towards PEA enantiomers, respectively.

The frequency changes were measured versus time as one of the chiral pairs was injected into the system to interact with **5(a/b)** on the QCM surface. Frequency changes of chiral calix[4]arene derivative coated QCM sensors towards PEA enantiomers are given in Table 1. There is a contrary interaction between a chiral analyte and

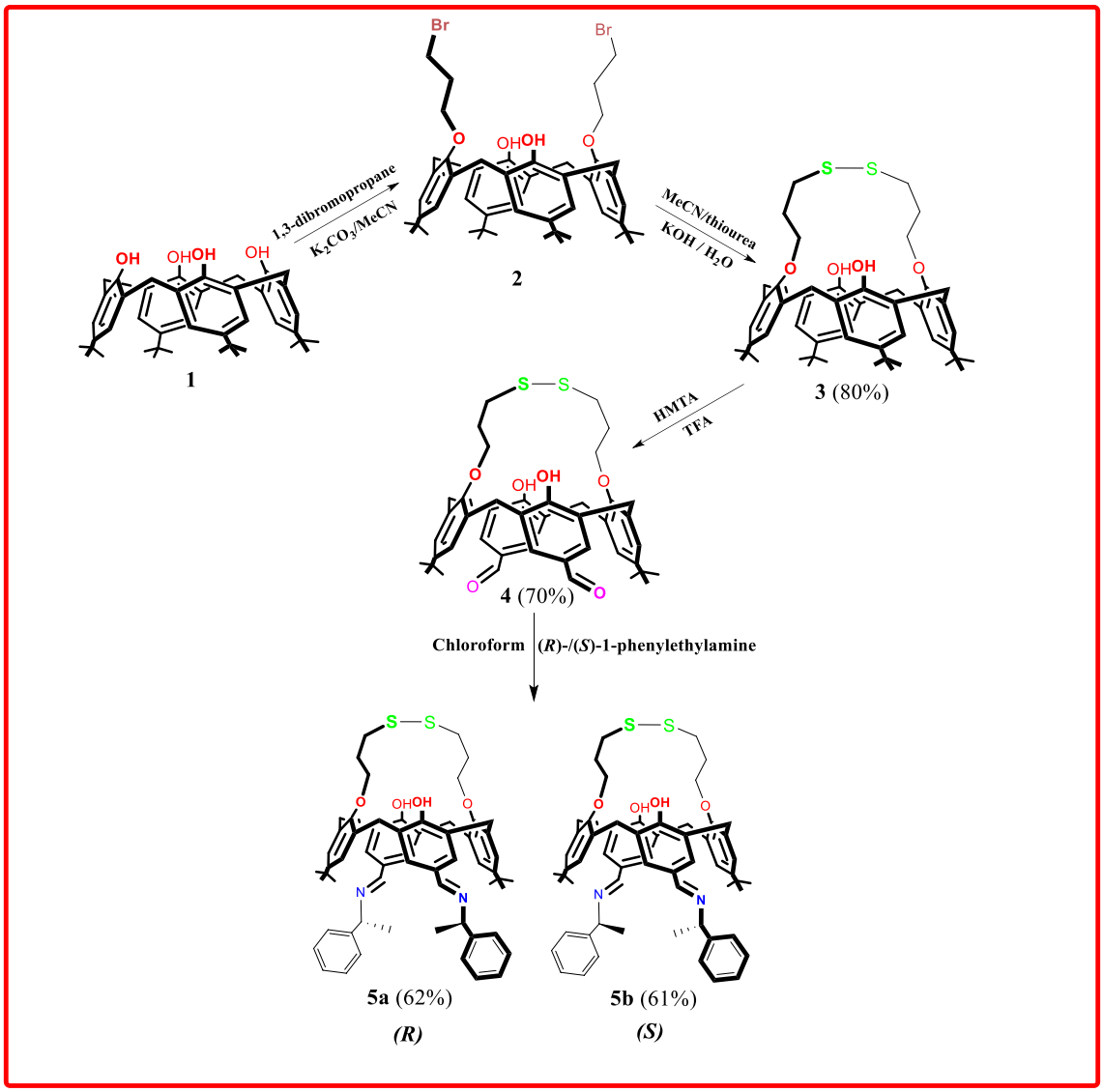

Scheme 1 Synthetic route of preparation of chiral compunds **5(a/b)**

chiral sensor molecules according to the principle of chiral recognition [33]. Frequency changes of **5a** coated QCM sensor towards PEA enantiomers are close to each other. On the other hand, frequency changes of **5b** coated QCM sensor towards PEA enantiomers are different from each other and it is more interested in (*R*)-PEA enantiomer. Enantiomeric discrimination factors were calculated for both sensors as 0.93 and 1.34 and were given in Table 1, respectively. Herein, it is a fact that the hydrogen bond interactions between the analyte and the chiral binding sites of sensing materials are the major factors in the chiral recognition. However, it is also clear that the different chiral orientations required by the nature of chirality are primarily responsible for the chiral discrimination phenomena.

Subsequent experiments were performed with **5b** coated QCM sensor due to its having relatively more chiral discrimination capability. So, it was tested towards PEA enantiomer solutions having different concentrations (10, 50, 100, 200 and 300 µM). As it seen in Fig. 3a, b, ΔF increased gradually as expected when the concentration of PEA enantiomer solutions was increased. Additionally, the calibration curves of frequency changes towards PEA enantiomer solutions in different concentrations were also given in Fig. 4a. However, sensor responses increased as linear by increasing of PEA concentration ($R^2 = 0.997$ for (*R*)-PEA and 0.997 for (*S*)-PEA). Furthermore, enantiomeric discrimination was increased due to the increasing of PEA concentrations in Fig. 4b. It was also noticed that enantiomeric discrimination increased almost linearly

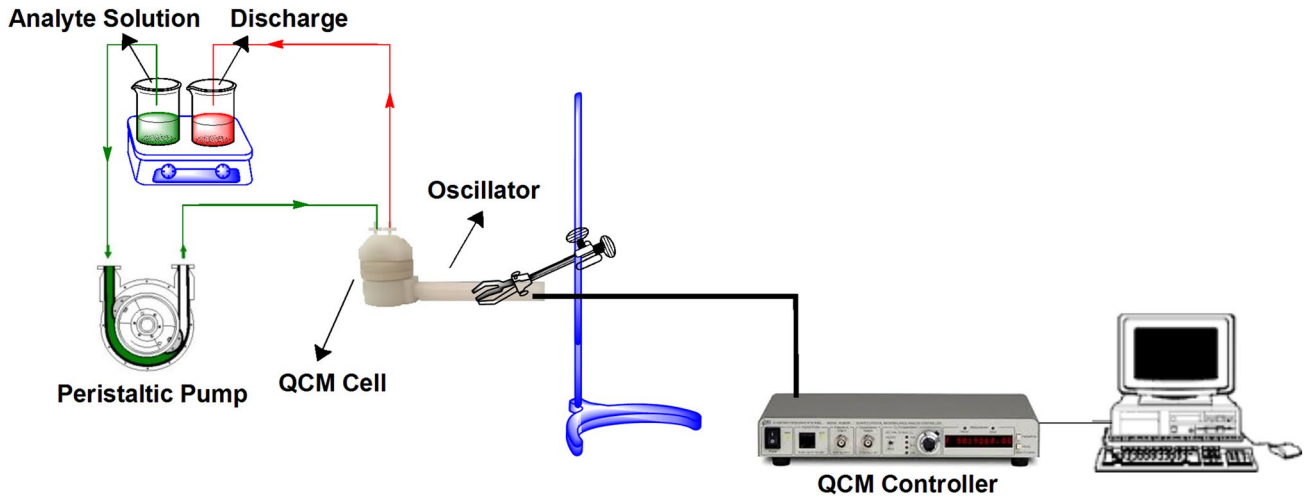

Fig. 2 Representation of QCM sensing system

Table 1 Frequency changes (−ΔHz) and enantiomeric discrimination factor (α) values of **5(a/b)** coated QCM sensors towards PEA enantiomers

Chiral sensing material	−ΔHz		α
	(R)-PEA	*(S)*-PEA	
5a *(R)*	8.2	8.8	0.93
5b *(S)*	15.7	11.7	**1.34**

[PEA]: 200 µM

beginning from 100 µM of PEA enantiomer solution while almost no enantiomeric discrimination was observed at lower concentrations.

Sensor sensitivity (*S*) can be easily determined from the slope of calibration curves which are drawn the frequency changes of sensor versus PEA enantiomers having different concentrations (in units of Hz μM^{-1}) [28]. DL of the sensor for chiral pairs were calculated using calibration curves of Fig. 4a by Eq. (3) [27]:

$$DL = 3\frac{S_{bl}}{m} \tag{3}$$

where S_{bl} is the standard deviation of the response, m is the slope of the calibration curve. Time constant (τ) values were also calculated for adsorption and desorption period of PEA enantiomers from the frequency changes of the sensor towards chiral pairs (300 µM) during adsorption and desorption processes (see ESM, Figs. S10, and S11, respectively) [29, 34]. Hence, sensing parameters such as sensitivities, DL and τ were listed in Table 2. DL values of PEA enantiomers by different enantiomeric recognition methods in literature with the current study were summarized and compared in Table 3. It may be observed that the detection of PEA by **5b** coated QCM sensor is comparable with other methods [24, 35–40].

Adsorption evaluation of PEA sensing

It is a fact that the sensing of PEA molecules depends on the interaction between the sensible film layer and analyte molecules. This interaction can be explained with adsorption *via* interactions such as hydrogen bonding between PEA molecules and chiral calixarene molecules on the QCM surface. Accordingly, we have investigated the sensing behaviors of **5b** modified QCM sensor towards PEA enantiomers with regards to adsorption. However, it seen in Table 2, the adsorption rates of PEA enantiomers are higher than their desorption rates. This case indicated that there was strong hydrogen bonding interaction between PEA molecules and chiral calixarene molecules. Hence, these interactions cannot easily destroyed by distilled water during desorption process so it could be occurred for a long time.

Many adsorption isotherms are applied to describe the adsorption mechanism in adsorption studies. Langmuir and Freundlich isotherms are the most common of them.

Langmuir isotherm is defined by the following equation [41]:

$$\frac{C_e}{q_e} = \frac{1}{q_0 b} + \frac{C_e}{q_0} \tag{4}$$

where C_e is equilibrium concentration (mg L^{-1}) in solution, q_e is adsorption capacity (mg mg^{-1}) at equilibrium, the constant q_0 indicates the adsorption capacity (mg mg^{-1}) and b is related to the energy of adsorption (L $mmol^{-1}$). The linear plot of C_e/q_e versus C_e shows that adsorption follows Langmuir isotherm for the sensing of PEA enantiomers (see

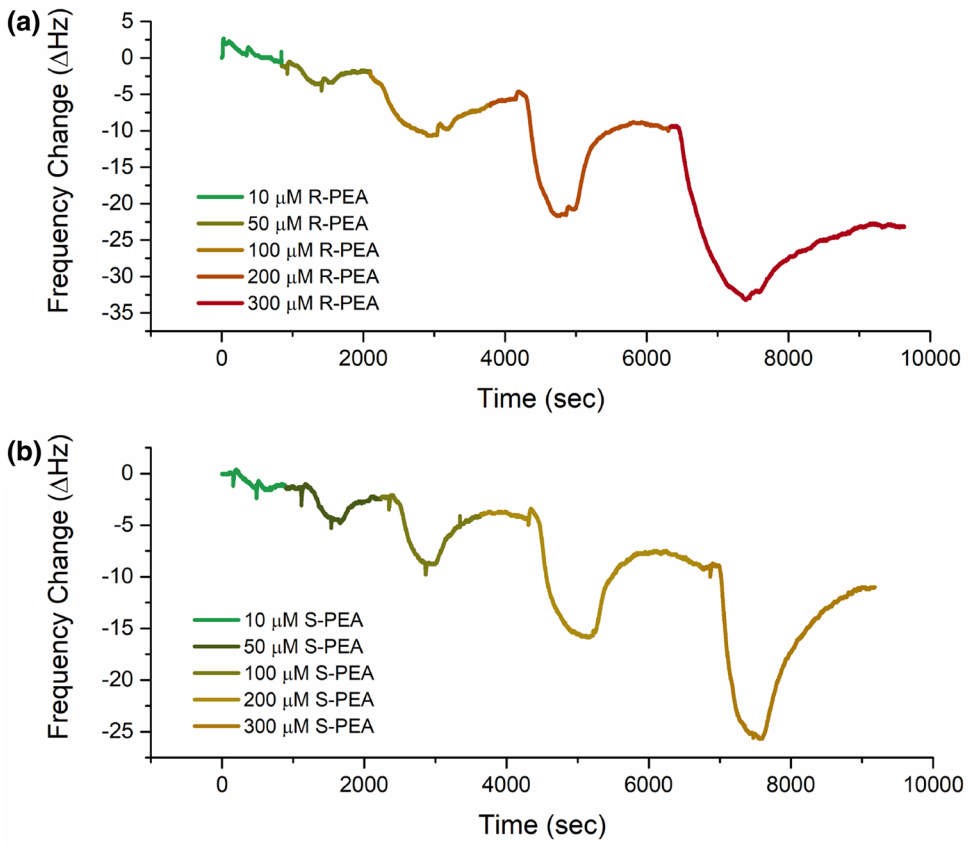

Fig. 3 Frequency changes of **5b** coated QCM sensor towards **a** (*R*)-PEA enantiomer in different concentrations and **b** (*S*)-PEA enantiomer in different concentrations

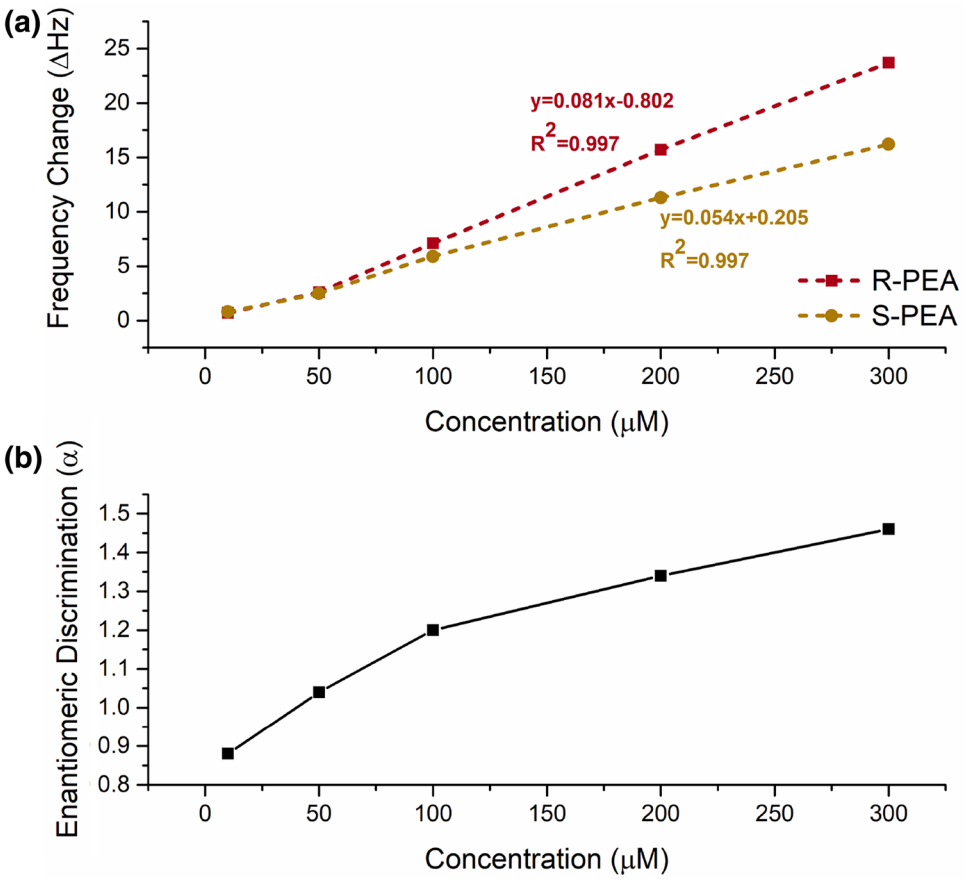

Fig. 4 **a** Calibration curve of frequency change towards PEA enantiomers and **b** enantiomeric discrimination factor (α) change of PEA enantiomer solutions in different concentration by using **5b** coated QCM sensor

Table 2 *DL*, *S* and τ values of **5b** coated QCM sensor for PEA enantiomer sensing

Enantiomers	*DL* (μM)	*S* (Hz/μM)	T_{ads} (s)[a]	τ_{des} (s)
(R)-PEA	2.7	0.082	319.2	1390.2
(S)-PEA	2.4	0.055	197.2	921.9

[a]It sign adsorption and desorption processes of 300 μM solutions of PEA enantiomers, respectively

ESM, Fig. S12). Values of q_0 and b were calculated from the slope and intercept of the linear plots and are given in Table 3.

To determine if the adsorption processes of PEA enantiomers by the QCM sensor are favorable or unfavorable for the Langmuir type adsorption process, the isotherm shape can be classified by a term "R_L" a dimensionless constant separation factor, which is defined below [42]:

$$R_L = \frac{1}{1 + bC_0} \tag{5}$$

where b is Langmuir constant (L mmol^{-1}). The parameter R_L indicates the shape of the isotherm accordingly: $R_L > 1$, unfavorable; $R_L = 1$, linear; $0 < R_L < 1$, favorable; $R_L = 0$, irreversible.

The calculated R_L values were also shown in Table 4. As a result of calculated R_L values, adsorption of PEA enantiomers by the QCM sensor was favorable at the range of 10–300 μM of initial PEA concentrations.

Besides, Freundlich isotherm was employed for adsorption of the PEA enantiomers by the sensor. Freundlich isotherm model is given by the following equation [43]:

$$\log q_e = \log K_f + (1/n) \log C_e \tag{6}$$

where K_f and n are Freundlich adsorption isotherm constants, being indicative of the adsorption capacity and intensity of adsorption. The values of K_f and n were calculated from the intercept and slope of the plots of $log\ q_e$ versus $log\ C_e$ (see ESM Fig. S13). Freundlich isotherm data are also given in Table 4.

The equilibrium dissociation constant was calculated by measuring frequency change according to different concentrations of PEA enantiomer in aqueous solution. Thus, Scatchard equilibrium isotherm model was applied to the sensing of chiral calix[4]arene coated QCM sensor towards PEA enantiomers by Eq. (7) [44]:

$$\frac{\Delta F}{C} = \frac{[(\Delta F_{max} - \Delta F)}{K_d} \tag{7}$$

where ΔF_{max} (Hz) is the maximum frequency change when all calix[4]arene molecules on QCM crystal were saturated, ΔF (Hz) is the frequency change at a specific PEA enantiomer concentration, C (mmol L^{-1}) is the concentration of PEA enantiomers, K_d (mmol L^{-1}) is the equilibrium dissociation constant. Scatchard analysis was carried out by plotting of $\Delta F/C$ versus ΔF. So, the K_d value was calculated by the slope of plot (see ESM, Fig. S14) as 0.753 mmol L^{-1} and 0.683 mmol L^{-1} for *(R)*-PEA and *(S)*-PEA, respectively (Table 4).

On the comparison of the R^2 values, we can conclude that Langmuir, Freundlich and Scatchard equations represent well fit to the experimental data in adsorption of PEA enantiomers on the surface of the sensor.

Table 3 Comparison of different enantiomeric recognition methods for PEA enantiomers in literature

Methods	Analytes	Linear concentration range	DL (μM)	References
Electrochemical	PEA	1–100 μM	1.3	[24]
Fluorescence	PEA	1.64–8.26 μM	–	[35]
Fluorescence	PEA	0–3 mM	–	[36]
CD spectroscopy	PEA	–	–	[37]
Optical micro-sensor	PEA	5–8 mM	–	[38]
Optical sensor	PEA	30 μM–100 mM	7–700	[39]
UV–Vis	PEA	124–701 μM	16.5	[40]
QCM	PEA	10–300 μM	2.4	Current study

Table 4 Isotherm data for the adsorption of PEA enantiomers from aqueous solution

Enantiomers	Langmuir				Freundlich			Scatchard		
	q_0 (mmol g^{-1})	b (L mmol^{-1})	R^2	R_L	K_f	n	R^2	K_d (mmol L^{-1})	ΔF_{max} (Hz)	R^2
(R)-PEA	4.721	1.348	0.999	$0 < R_L < 1$	5.987	1.014	0.997	0.753	61.19	0.999
(S)-PEA	3.772	1.467	0.998	$0 < R_L < 1$	6.100	1.122	0.996	0.683	48.27	0.993

Effect of calixarene content

It was prepared the QCM sensors which have various mass loadings of the **5b** on QCM surface. Thus, we have examined the effect of calixarene substance on enantiomeric discriminations of 200 µM PEA enantiomers. It was observed an alteration at mass loading of QCM sensors and enantiomeric discrimination factor as the **5b** subtance was changing on QCM sensor. This revealed that the **5b** content played an important role in sensing process. Mass loadings of QCM sensors and enantiomeric discriminations of PEA enantiomers were given in Fig. 5. As it seen in Fig. 5, as mass loading of QCM sensors increase so enantiomeric discriminations increased gradually as expected.

Effect of coating technique

Spin coating and drop casting technique were used as well as soaking technique to demonstrate the effect of coating technique on enantiomeric discrimination of PEA enantiomers. The coating of the chiral calix[4]arene derivatives by soaking technique onto QCM surface was given previously in this study. After coating, the mass loading of **5b** on QCM surface was determined as 78 Hz. For the coating of **5b** on QCM surface by spin technique, 100 µL of **5b** solution (1 mM, in chloroform) was used at 1000 rpm and 30 s, and the mass loading of the **5b** on QCM surface was determined as 72 Hz. For the coating of the **5b** by drop technique on QCM surface, 20 µL of **5b** solution (1 mM, in chloroform) was applied to surface, and solvent evaporated at 60 °C for 30 min in drying-oven to obtain **5b** modified QCM sensor. After coating, the mass loading of **5b** on QCM crystal surface was determined as 195 Hz. For the evidence to depositions of **5b** on QCM sensor, contact angle measurements were performed. As it seen in Fig. 6, contact angles of bare crystal surface and **5b** modified QCM sensor surfaces by soaking, spin coating and drop casting technique were measured as 68°, 94.5°, 81.7° and 86.3°, respectively. The surface can be classified as high wettability ($\theta \ll 90°$) or low wettability ($\theta \gg 90°$) in terms of contact angle [45]. Hence, the increase of contact angle value on bare crystal surface and hydrophobic moieties of calix[4]arenes indicated that **5b** were successfully deposited on QCM sensor by all deposition techniques. According to the contact angles of **5b** modified QCM sensors, it was seen that soaking technique was more efficient in spreading of **5b** molecules on QCM sensor than others.

Moreover, AFM images of QCM sensors were taken to evaluate changing of their surface morphologies after deposition. AFM in semi-contact mode was applied to characterize the formation of **5b** modified QCM sensors on the gold surface by different coating techniques.

AFM images of the bare crystal surface and the **5b** modified QCM sensors by soaking, spin coating and drop casting techniques were given in Fig. 7, respectively. The root mean square roughness increased with each layer, from 2.14 nm for bare crystal surface to 4.82 nm for **5b** modified QCM sensor by soaking technique, 4.81 nm for **5b** modified QCM sensor by spin coating technique and 35.99 nm for **5b** modified QCM sensor by drop casting technique. The increase of peak-to-peak height (bare crystal surface 27.91 nm, soaking method 48.03 nm, spin coating 39.55 nm and drop casting 237.181 nm) indicated the formation of **5b** modified QCM

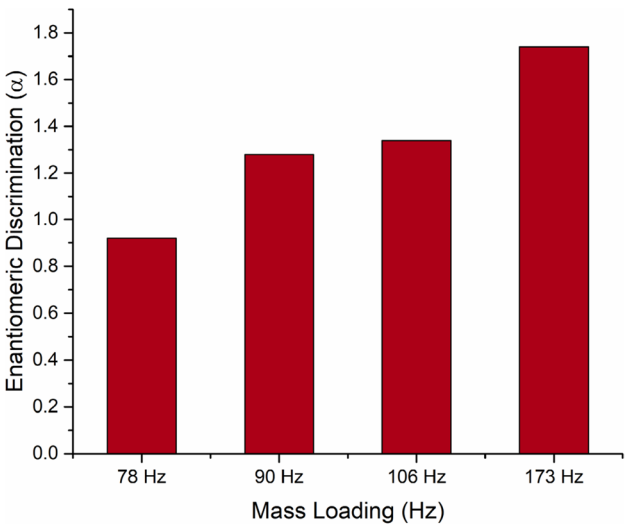

Fig. 5 Enantiomeric discrimination factor (α) of PEA enantiomers by **5b** coated QCM sensors having different mass loadings

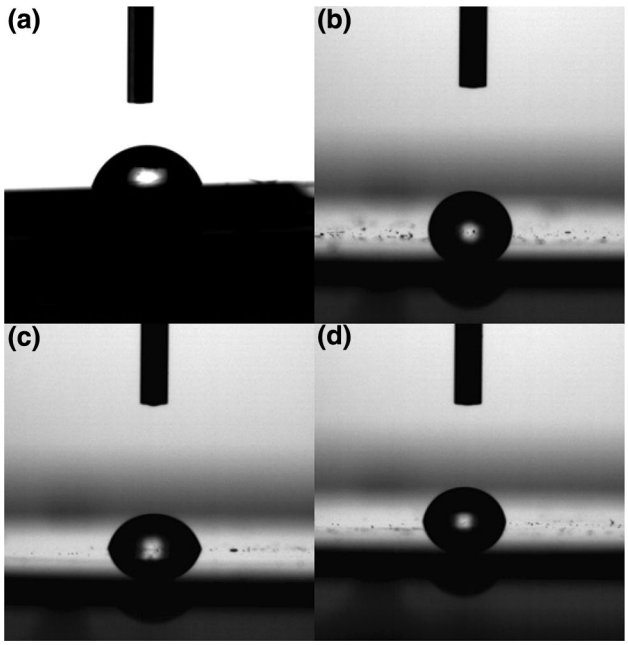

Fig. 6 Contact angle images of **a** bare gold surface, **5b** coated QCM sensors by **b** soaking, **c** spin coating, and **d** drop casting

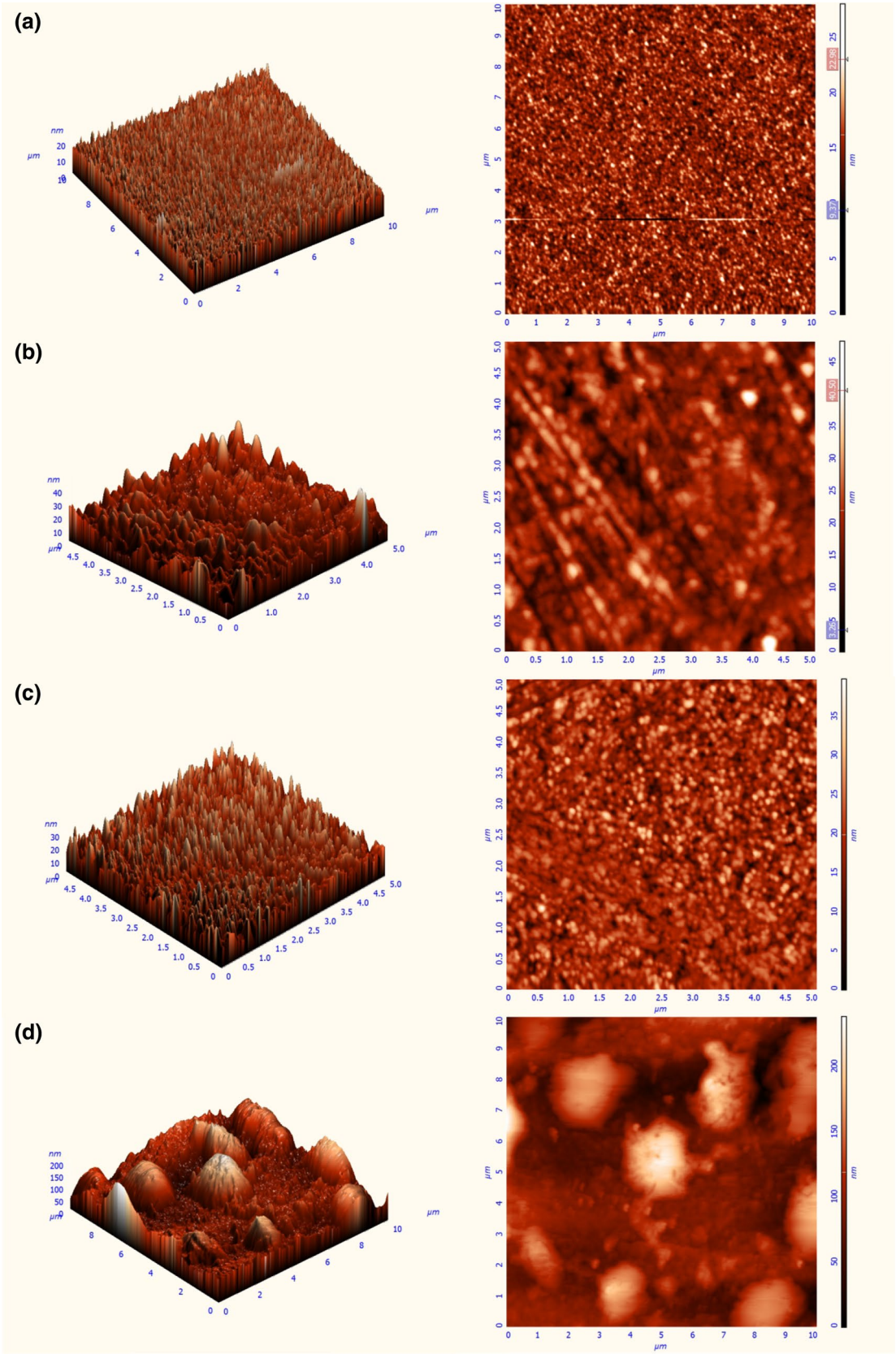

Fig. 7 AFM images of **a** bare gold surface, **5b** coated QCM sensors by **b** soaking, **c** spin coating and **d** drop casting

sensors on bare crystal surface by each techniques. Thus, the bond formation between disulfide moieties of **5b** molecules and gold on bare crystal surface resulted in the formation of **5b** modified QCM sensors.

Furthermore, the bare gold crystal surface seems to be almost smooth as expected. At the end of coating, many large peaks are seen on surfaces in Fig. 8. Indeed, different surface morphologies can be explicitly observed from each coating techniques for the preparing of **5b** modified QCM sensors. The surface of **5b** modified QCM sensor by soaking technique (in Fig. 8b) has some large peaks which are not same height and wideness. This implies that **5b** molecules may be settled untidy and/or overlapped each other. In case of spin coating, the surface of **5b** modified QCM sensor (in Fig. 8c) was almost smooth. This case indicates that **5b** molecules can be scattered on QCM sensor surface coequally but there are some gaps locally. In case of drop casting coating, the surface of **5b** modified QCM sensor (in Fig. 8d) had no uniform morphology. There were some height and large peaks in some places of surface.

Table 5 shows enantiomeric discrimination factors for PEA enantiomers by the QCM sensors which are fabricated by different coating techniques and mass loading of these QCM sensors. Although the enantiomeric discrimination for PEA enantiomers by the QCM sensor which is modified by soaking technique is higher than it by drop casting technique, the enantiomeric discrimination for PEA enantiomers by the QCM sensor which is modified by spin technique is higher than it by soaking technique. In generally, when all coating techniques compared each other in terms of enantiomeric discrimination for PEA enantiomers, soaking technique can be selected as most favorable coating technique for an efficient enantiomeric discrimination. This can be attributed to somewhat more suitable spreading of **5b** on QCM sensor surface by soaking technique.

Table 5 Comparison of different coating techniques in terms of frequency change (−ΔHz) and enantiomeric discrimination factor (α) values of **5b** modified QCM sensor

Coating technique	Mass loading (Hz)	Frequency change (Hz)		α
		(*R*)-PEA	(*S*)-PEA	
Soaking	173	7.3	4.2	0.34
Drop casting	195	5.5	6.8	0.19
Soaking	78	8	8.7	0.08
Spin coating	72	6.3	5.5	0.15

[PEA]: 200 µM

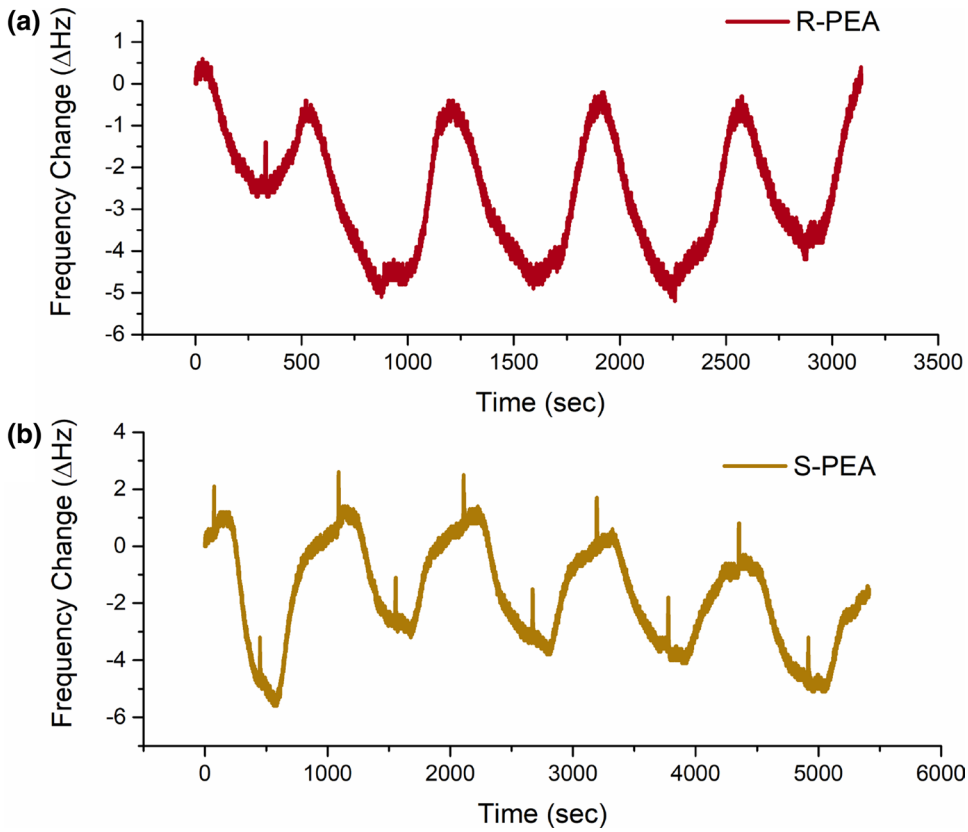

Fig. 8 Repeatability test of **5b** coated QCM sensor towards **a** (*R*)-PEA in terms of frequency changes and **b** (*S*)-PEA in terms of frequency changes

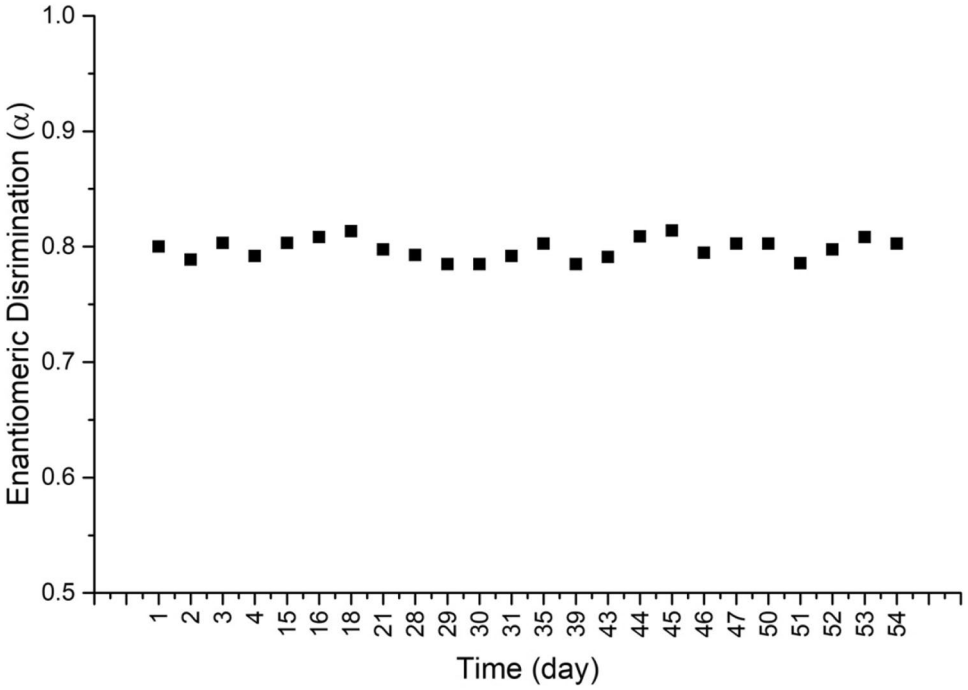

Fig. 9 Durability test of **5b** coated QCM sensor towards PEA enantiomers

Repeatability and durability of sensor

It is well known that the repeatability and the durability of a sensor are very important parameters in sensing studies. In order to examine the repeatability of **5b** modified QCM sensor (106 Hz of mass loading by soaking technique), it was exposed to solution of PEA enantiomers (50 µM) at least five times, and ΔF values were recorded and given in Fig. 8. After every adsorption and desorption process were performed by distilled water (DW). The results demonstrated that **5b** modified QCM sensor showed a superior repeatability in sensing of PEA enantiomers.

To measure the durability of **5b** modified QCM sensor, frequency changes were recorded after the QCM sensor exposed to solution of the PEA enantiomers (50 µM) in different time intervals. The results (Fig. 9) showed that there was not performed significant difference in existent enantiomeric discrimination of PEA enantiomers during 2 months. This result imply the fact that **5b** modified QCM sensor can be useful for a long time in enantiomeric recognition operations.

Conclusion

In this study, a series of chiral calix[4]arene coated QCM sensors was generated for applying to enantiomeric discriminations of PEA enantiomers. **5b** coated QCM sensor exhibited highest enantiomeric discrimination ability towards PEA enantiomers. It was considered that hydrogen bonding capabilities and chiral properties of sensing materials were major factors during enantioselective sensing process. It has been calculated that the sensitivity and DL values 0.082 Hz μM^{-1} and 2.7 µM, respectively. Thus, it has been produced a new QCM sensor for PEA enantiomers having outstanding properties such as real-time, sensitive, effective and enantioselective detection, durable and recoverable with DW by this work. It has been concluded that calixarenes are more suitable and promising candidate materials for chiral separation of amine enantiomers as combined with a QCM sensing system. Accordingly, this approach can be used in applications on sensor technologies and contributes to new studies in terms of discrimination of racemic mixtures.

Acknowledgements We thank the Technical Research Council of Turkey (TUBITAK—Grant No. 115Z249) and the Research Foundation of the Selçuk University (SUBAP-Grant No. 16401003), Konya, Turkey and for financial support of this work produced from Egemen Ozcelik's M.Sc. Thesis.

References

1. Zhou, Y., Ren, Y., Zhang, L., You, L., Yuan, Y., Anslyn, E.V.: Dynamic covalent binding and chirality sensing of mono secondary amines with a metal-templated assembly. Tetrahedron **71**(21), 3515–3521 (2015)
2. Kodamatani, H., Iwaya, Y., Saga, M., Saito, K., Fujioka, T., Yamazaki, S., Kanzaki, R., Tomiyasu, T.: Ultra-sensitive HPLC-photochemical reaction-luminol chemiluminescence method for the measurement of secondary amines after nitrosation. Anal. Chim. Acta **952**, 50–58 (2017)

3. Jennings, K., Diamond, D.: Enantioselective molecular sensing of aromatic amines using tetra-(S)-di-2-naphthylprolinol calix[4] arene. Analyst **126**(7), 1063–1067 (2001)
4. Stringham, R.W., Ye, Y.K.: Chiral separation of amines by high-performance liquid chromatography using polysaccharide stationary phases and acidic additives. J. Chromatogr. A **1101**(1), 86–93 (2006)
5. Zhang, Y., Woods, R.M., Breitbach, Z.S., Armstrong, D.W.: 1,3-Dimethylamylamine (DMAA) in supplements and geranium products: natural or synthetic? Drug Test. Anal. **4**(12), 986–990 (2012)
6. Tabakci, M., Tabakci, B., Yilmaz, M.: Design and synthesis of new chiral calix[4]arenes as liquid phase extraction agents for α-amino acid methylesters and chiral α-amines. J. Incl. Phenom. Macrocycl. Chem. **53**(1–2), 51–56 (2005)
7. Huang, Z., Yu, S., Zhao, X., Wen, K., Xu, Y., Yu, X., Xu, Y., Pu, L.: A convenient fluorescent method to simultaneously determine the enantiomeric composition and concentration of functional chiral amines. Chemistry **20**(50), 16458–16461 (2014)
8. Mishra, S.K., Chaudhari, S.R., Lakshmipriya, A., Pal, I., Lokesh, N., Suryaprakash, N.: Novel synthetic as well as natural auxiliaries with a blend of NMR methodological developments for chiral analysis in isotropic media. In Annual Reports on NMR Spectroscopy, Vol. **91**, pp. 143–292. Academic Press, Cambridge (2017)
9. Guo, L., Wang, D., Xu, Y., Qiu, B., Lin, Z., Dai, H., Yang, H.H., Chen, G.: Discrimination of enantiomers based on LSPR biosensors fabricated with weak enantioselective and nonselective receptors. Biosens. Bioelectron. **47**, 199–205 (2013)
10. Kertész, J., Huszthy, P., Kormos, A., Bertha, F., Horváth, V., Horvai, G.: Synthesis of new optically active acridino-18-crown-6 ligands and studies of their potentiometric selectivity toward the enantiomers of protonated 1-phenylethylamine and metal ions. Tetrahedron **20**(24), 2795–2801 (2009)
11. Wang, L., Zhang, Y., Wu, A., Wei, G.: Designed graphene-peptide nanocomposites for biosensor applications: a review. Anal. Chim. Acta **985**, 24–40 (2017)
12. March, C., Garcia, J.V., Sanchez, A., Arnau, A., Jimenez, Y., Garcia, P., Manclus, J.J., Montoya, A.: High-frequency phase shift measurement greatly enhances the sensitivity of QCM immunosensors. Biosens. Bioelectron. **65**, 1–8 (2015)
13. Montmeat, P., Veignal, F., Methivier, C., Pradier, C.M., Hairault, L.: Study of calixarenes thin films as chemical sensors for the detection of explosives. Appl. Surf. Sci. **292**, 137–141 (2014)
14. Pei, Z., Saint-Guirons, J., Kack, C., Ingemarsson, B., Aastrup, T.: Real-time analysis of the carbohydrates on cell surfaces using a QCM biosensor: a lectin-based approach. Biosens. Bioelectron. **35**(1), 200–205 (2012)
15. Karaseva, N., Ermolaeva, T., Mizaikoff, B.: Piezoelectric sensors using molecularly imprinted nanospheres for the detection of antibiotics. Sens. Actuators B **225**, 199–208 (2016)
16. Jearanaikoon, P., Prakrankamanant, P., Leelayuwat, C., Wanram, S., Limpaiboon, T., Promptmas, C.: The evaluation of loop-mediated isothermal amplification-quartz crystal microbalance (LAMP-QCM) biosensor as a real-time measurement of HPV16 DNA. J. Virol. Methods **229**, 8–11 (2016)
17. Hao, R.Z., Song, H.B., Zuo, G.M., Yang, R.F., Wei, H.P., Wang, D.B., Cui, Z.Q., Zhang, Z., Cheng, Z.X., Zhang, X.E.: DNA probe functionalized QCM biosensor based on gold nanoparticle amplification for *Bacillus anthracis* detection. Biosens. Bioelectron. **26**(8), 3398–3404 (2011)
18. Sauerbrey, G.: Verwendung von Schwingquarzen zur Wägung dünner Schichten und zur Mikrowägung. Zeitschrift für Physik **155**(2), 206–222 (1959)
19. Tabakci, M.: Immobilization of calix[6]arene bearing carboxylic acid and amide groups on aminopropyl silica gel and its sorption properties for Cr(VI). J. Incl. Phenom. Macrocycl. Chem. **61**(1), 53–60 (2008)
20. Temel, F., Tabakci, M.: Calix[4]arene coated QCM sensors for detection of VOC emissions: methylene chloride sensing studies. Talanta **153**, 221–227 (2016)
21. Temel, F., Ozcelik, E., Ture, A.G., Tabakci, M.: Sensing abilities of functionalized calix[4]arene coated QCM sensors towards volatile organic compounds in aqueous media. Appl. Surf. Sci. **412**, 238–251 (2017)
22. Kostyukevych, K.V., Khristosenko, R.V., Pavluchenko, A.S., Vakhula, A.A., Kazantseva, Z.I., Koshets, I.A., Shirshov, Y.M.: A nanostructural model of ethanol adsorption in thin calixarene films. Sens. Actuators B **223**, 470–480 (2016)
23. Juaristi, E., León-Romo, J.L., Reyes, A., Escalante, J.: Recent applications of α-phenylethylamine (α-PEA) in the preparation of enantiopure compounds. Part 3: α-PEA as chiral auxiliary. Part 4: α-PEA as chiral reagent in the stereodifferentiation of prochiral substrates[1]. Tetrahedron **10**(13), 2441–2495 (1999)
24. Kuang, R., Zheng, L., Chi, Y., Shi, J., Chen, X., Zhang, C.: Highly efficient electrochemical recognition and quantification of amine enantiomers based on a guest-free homochiral MOF. RSC Adv. **7**(19), 11701–11706 (2017)
25. Breuer, M., Ditrich, K., Habicher, T., Hauer, B., Keßeler, M., Stürmer, R., Zelinski, T.: Industrial methods for the production of optically active intermediates. Angew. Chem. Int. Ed. **43**(7), 788–824 (2004)
26. Su, W.C., Zhang, W.G., Zhang, S., Fan, J., Yin, X., Luo, M.L., Ng, S.C.: A novel strategy for rapid real-time chiral discrimination of enantiomers using serum albumin functionalized QCM biosensor. Biosens. Bioelectron. **25**(2), 488–492 (2009)
27. Long, G.L., Winefordner, J.D.: Limit of detection a closer look at the IUPAC definition. Anal. Chem. **55**(07), 712A–724A (1983)
28. Koshets, I.A., Kazantseva, Z.I., Belyaev, A.E., Kalchenko, V.I.: Sensitivity of resorcinarene films towards aliphatic alcohols. Sens. Actuators B **140**(1), 104–108 (2009)
29. Fu, Y., Finklea, H.O.: Quartz crystal microbalance sensor for organic vapor detection based on molecularly imprinted polymers. Anal. Chem. **75**(20), 5387–5393 (2003)
30. Li, Z.-T., Ji, G.-Z., Zhao, C.-X., Yuan, S.-D., Ding, H., Huang, C., Du, A.-L., Wei, M.: Self-assembling calix[4]arene [2]catenanes. Preorganization, conformation, selectivity, and efficiency. J. Org. Chem. **64**(10), 3572–3584 (1999)
31. Gutsche, C.D., Dhawan, B., No, K.H., Muthukrishnan, R.: Calixarenes. 4. The synthesis, characterization, and properties of the calixarenes from p-tert-butylphenol. J. Am. Chem. Soc. **103**(13), 3782–3792 (1981)
32. Chawla, H.M., Pant, N., Srivastava, B., Upreti, S.: Convenient direct synthesis of bisformylated calix[4]arenes via ipso substitution. Org. Lett. **8**(11), 2237–2240 (2006)
33. Nakanishi, T., Yamakawa, N., Asahi, T., Shibata, N., Ohtani, B., Osaka, T.: Chiral discrimination between thalidomide enantiomers using a solid surface with two-dimensional chirality. Chirality **16**, S36–S39 (2004)
34. Grate, J.W., Snow, A., Ballantine, D.S., Wohltjen, H., Abraham, M.H., McGill, R.A., Sasson, P.: Determination of partition coefficients from surface acoustic wave vapor sensor responses and correlation with gas-liquid chromatographic partition coefficients. Anal. Chem. **60**(9), 869–875 (1988)
35. Upadhyay, S.P., Pissurlenkar, R.R.S., Coutinho, E.C., Karnik, A.V.: Furo-fused BINOL based crown as a fluorescent chiral sensor for enantioselective recognition of phenylethylamine and ethyl ester of valine. J. Org. Chem. **72**(15), 5709–5714 (2007)
36. Grady, T., Harris, S.J., Smyth, M.R., Diamond, D., Hailey, P.: Determination of the enantiomeric composition of chiral amines based on the quenching of the fluorescence of a chiral calixarene. Anal. Chem. **68**(21), 3775–3782 (1996)

37. Yang, Y., Pei, X.-L., Wang, Q.-M.: Postclustering dynamic covalent modification for chirality control and chiral sensing. J. Am. Chem. Soc. **135**(43), 16184–16191 (2013)
38. Charrier, J., Brandily, M.-L., Lhermite, H., Michel, K., Bureau, B., Verger, F., Nazabal, V.: Evanescent wave optical micro-sensor based on chalcogenide glass. Sens. Actuators B **173**, 468–476 (2012)
39. He, H., Uray, G., Wolfbeis, O.S.: Enantioselective optodes. Anal. Chim. Acta **246**(2), 251–257 (1991)
40. Gazzani, G., Stoppini, G., Gandini, C., Bettero, A.: Reversed-phase high-performance liquid chromatographic and derivative UV spectrophotometric determination of α-phenylethylamine in phosphomycin. J. Chromatogr. A **609**(1), 391–394 (1992)
41. Weber, W.J.: Physicochemical Processes for Water Quality Control. Wiley, New York (1972)
42. Hamdaoui, O.: Dynamic sorption of methylene blue by cedar sawdust and crushed brick in fixed bed columns. J. Hazard. Mater. **138**(2), 293–303 (2006)
43. Rao, M., Parwate, A.V., Bhole, A.G.: Removal of Cr^{6+} and Ni^{2+} from aqueous solution using bagasse and fly ash. Waste Manag. **22**(7), 821–830 (2002)
44. Bayramoglu, G., Ozalp, C., Oztekin, M., Guler, U., Salih, B., Arica, M.Y.: Design of an aptamer-based magnetic adsorbent and biosensor systems for selective and sensitive separation and detection of thrombin. Talanta **191**, 59–66 (2019)
45. Yuan, Y., Lee, T.R.: Contact Angle and Wetting Properties. In: Bracco, G., Holst, B. (eds.) Surface Science Techniques, pp. 3–34. Springer, Berlin (2013)